






LETTER | JUNE 02 2022

## Assessing effectiveness and comfortability of a two-layer cloth mask with a high-efficiency particulate air (HEPA) insert to mitigate COVID-19 transmission

SCI F FREE

Special Collection: [Flow and the Virus](#)

Yagya Narayan ; Sanghamitro Chatterjee; Amit Agrawal  ; Rajneesh Bhardwaj  



*Physics of Fluids* 34, 061703 (2022)

<https://doi.org/10.1063/5.0094116>



View  
Online



Export  
Citation

CrossMark

### Articles You May Be Interested In

HEPA filter improves homemade cloth mask to surgical mask standards

*Scilight* (June 2022)

A comprehensive study on respiratory parameters using bluetooth enabled multilayered COVID mask: A preventive measure

*AIP Conference Proceedings* (April 2023)

An apparatus for rapid and nondestructive comparison of masks and respirators

*Rev. Sci. Instrum.* (November 2020)

# Assessing effectiveness and comfortability of a two-layer cloth mask with a high-efficiency particulate air (HEPA) insert to mitigate COVID-19 transmission

Cite as: Phys. Fluids **34**, 061703 (2022); doi: 10.1063/5.0094116

Submitted: 1 April 2022 · Accepted: 10 May 2022 ·

Published Online: 2 June 2022






View Online



Export Citation



CrossMark

Yagya Narayan,  Sanghamitro Chatterjee, Amit Agrawal,  and Rajneesh Bhardwaj 

## AFFILIATIONS

Department of Mechanical Engineering, Indian Institute of Technology Bombay, Mumbai 400076, India

Note: This paper is part of the special topic, Flow and the Virus.

<sup>a)</sup>Authors to whom correspondence should be addressed: [rajneesh.bhardwaj@iitb.ac.in](mailto:rajneesh.bhardwaj@iitb.ac.in) and [amit.agrawal@iitb.ac.in](mailto:amit.agrawal@iitb.ac.in)

## ABSTRACT

A face mask is essential personal protective equipment to mitigate the spread of COVID-19. While a cloth mask has the least ability to prevent the passage of infectious respiratory droplets through it compared to surgical and N95 masks, the surgical mask does not fit snugly and causes significant air leakage. The synthetic fibers in the latter reduce comfortability and are an allergen for facial eczema. Moreover, the N95 mask causes CO<sub>2</sub> inhalation and reduces heat transfer in the nose. Therefore, the objective of the present work is to improve the effectiveness of a two-layer cloth mask by introducing an intermediate, high-efficiency particulate air (HEPA) filter layer. A significant volume of impacted droplets penetrates through a single-layer cloth mask, ejecting secondary droplets from the rear side. However, a two-layer cloth mask prevents this ejection. Despite slowing down the liquid penetration, capillary imbibition through cloth due to its hydrophilicity causes the transport of the liquid into the second layer, resulting in a thin-liquid layer at the mask's rear-side surface and contaminating it. Conversely, the HEPA filter inserted in the cloth mask prevents the imbibition, making the second cloth layer free of contamination. We attribute the impediment to the imbibition by the intermediate HEPA filter layer to its hydrophobic characteristics. We experimentally and analytically assess the role of wettability on capillary imbibition. The breathability measurements of masks show that the HEPA inserted in the cloth mask does not reduce its breathability compared to that of the surgical mask.

Published under an exclusive license by AIP Publishing. <https://doi.org/10.1063/5.0094116>

There has been a growing consensus among the researchers that respiratory droplets are the main vector in the transmission of the coronavirus disease (COVID-19) caused by Severe Acute Respiratory Syndrome Coronavirus-2 (SARS-CoV-2).<sup>1–5</sup> Advanced studies revealed that the rotational diffusivity of the virion particles determines the dynamics of attack on the host cell.<sup>6,7</sup> There are three main routes of disease transmission briefed as follows:<sup>8</sup> (1) Direct exposure of the susceptible individual to the virus-laden respiratory droplets exhaled by an infected individual;<sup>9</sup> (2) Inhalation of virion containing small aerosolized droplets of size  $\leq 5 \mu\text{m}$  that remain suspended in the air for an extended period of time and undergo slower evaporation;<sup>10–14</sup> and (3) The infectious respiratory droplets, especially the heavier droplets, deposit on disparate surfaces to form *fomites*, and consequently, the surface becomes a secondary source of disease transmission; wherein the virus survival on the surface significantly depends upon the physical

and compositional properties of the surface.<sup>15–18</sup> There is mounting evidence that suggests that among the routes mentioned above, the first one is the predominant route of disease transmission.<sup>19</sup> The second route is typically responsible for disease spread in indoor spaces having poor ventilation.<sup>12</sup> The fomite route of disease is less dominant. However, the potential threat cannot be ruled out to assess the absolute risk of infection spread. To date, there is no consolidated evidence-based data to conclude about the relative importance of the fomite route in determining the disease spread;<sup>20</sup> however, it is believed that the fomite route of transmission is particularly prominent in typical settings such as hospitals and public gathering/waiting halls.<sup>21</sup> Therefore, hand hygiene and sanitization of frequently-touched surfaces are recommended by the World Health Organization (WHO).<sup>22</sup>

Experts are unanimous in their views that a face mask is an essential personal protective equipment for mitigation of the spread of

COVID-19.<sup>10,23,24</sup> The efficiency of face masks has been demonstrated based on the blockage of exhaled cough cloud, thereby reducing the propagation distance from the source and the volume of air entrained within by the cloud.<sup>10,25–29</sup> The three most popular face masks are cloth masks, surgical masks, and N95 masks. Researchers have demonstrated that cloth masks have the least capability of blocking the exhaled respiratory droplets.<sup>30</sup> While the blocking ability of surgical masks is higher, it does not snugly fit the face, and leakage of infectious cough cloud happens through the edges.<sup>30</sup> Among the three types of face masks, N95 masks are having the highest capability of inhibiting the passage of the respiratory fluid through them,<sup>31</sup> reducing the distance traveled by the ejected cough cloud from an individual's mouth.

Apart from the ability to block the passage of pathogen-containing respiratory fluids, the comfortability of a face mask is a crucial requirement,<sup>32,33</sup> owing to the need for its prolonged and constant usage as the pandemic wave continues to hit different parts of the world. As will be discussed later, the inner layer of a surgical mask is composed of a fibrous synthetic material. Hence, the fibers enter inside the nose, causing reduced breathing comfort. The material may be severely detrimental to the users who have a latex allergy, causing them to suffer from facial eczema.<sup>34,35</sup> N95 masks may also cause facial eczema stemming from a latex allergy, as suggested by recent measurements.<sup>36</sup> Furthermore, a significant number of frontline health workers reported adverse skin reactions, including acne, facial itch, and rash after prolonged use of N95 masks.<sup>37–39</sup> In addition, Computational Fluid Dynamics (CFD)-based studies have predicted that the N95 mask may cause excessive inhalation of CO<sub>2</sub> and reduced heat transfer in the human nasal cavity.<sup>40,41</sup> While CFD-based predictions remain to be experimentally validated, they have alerted the scientific community about the need for further research in the direction of developing protective face masks with sufficient breathability. On the other hand, masks with exhalation valves have reduced efficiency as the pathogen containing droplets pass through the valve, as shown by the recent measurements.<sup>28</sup> Thus, it is imperative to improve the efficiency of cloth masks. The cloth masks can be made of desired fabric, which does not cause facial eczema to allergic individuals. It can also be made with the desired size, which may tightly fit the face, an essential requirement, especially for juveniles. Furthermore, cloth masks may be considered to be less expensive. Therefore, the goal of the present investigation is to enhance the effectiveness of cloth masks.

Recent experimental, numerical, and analytical studies have shown that studying the interaction of a water droplet, as a surrogate to a respiratory droplet, with face masks<sup>42–44</sup> and face shields<sup>45</sup> is a powerful, yet more straightforward tool to evaluate the performance of the personal protective equipment under consideration. Importantly, since the aqueous phase of the respiratory droplet serves as a medium for the survival of enveloped viruses such as coronavirus,<sup>46,47</sup> the drying timescale of a water droplet and a residual thin-film on a surface are well correlated with the decay timescale of the virus titer on an inoculated surface.<sup>16–18</sup> The same concept has been applied in the present study to demonstrate proof-of-concept measurements and an analytical model to evaluate a distinctly designed cloth mask.

This work builds upon the previous works by Sharma *et al.*<sup>43</sup> and Krishnan *et al.*,<sup>44</sup> who investigated the impact and the associated consequences of a surrogate respiratory droplet on single to multiple layered surgical masks and home-made cloth masks, respectively. They showed that secondary droplet ejection occurs as the impacting

droplet impinges through the layers depending on the impact speed. In the case of surgical masks, while a significant volume of the impacting droplet is penetrated through single and double-layered masks, no penetration occurs through a triple-layer mask even at the highest impact speed. For the case of cloth, a significant penetration and emergence of secondary droplets were observed through a single layer. Based upon these observations, some specific questions remain, which we attempt to answer herein. (1) An essential characteristic of a porous medium is that capillary imbibition of deposited liquids occurs through the pores. Whether and how the secondary droplets generated from the first layer of a mask are imbibed through the successive layers remains unanswered. For instance, a multi-layered face mask may prevent the ejection of secondary droplets after the last layer; however, the question remains: does the rear-side surface of the mask get inoculated due to capillary imbibition of the secondary droplets through the layers? (2) How different are the capillary imbibition characteristics on cloth and surgical mask material? Among a two-layer cloth mask and three-layer surgical mask, whose rear-side surface gets contaminated due to the capillary imbibition of the secondary droplets? (3) Finally, we ask the principle research question of the present study: how to improve the efficiency of the homemade face masks, in the context of question (2) above? This is due to the fact that rustic cloths made of woven fabrics are well-known materials for exhibiting capillary imbibition.<sup>17</sup> As will be discussed later, in the experiments, we observe that a single-layer cloth mask allows a significant volume of the impacting droplet to penetrate through it generating secondary droplet ejection from the rear side. In contrast, a two-layer cloth mask prevents penetration of liquid and the associated generation of secondary droplets [cf. Figs. 7 (Multimedia view), 8 (Multimedia view), and 14]. While the liquid propagation slows down during passage through a double-layer cloth mask, capillary imbibition of the droplet-liquid through the second layer causes the formation of a thin layer of pathogen-bearing liquid on the rear-side surface of the second layer. Since the rear-side surface is exposed to the susceptible individual, it may serve as a potential source of disease spread. Based upon this observation, herein we seek to ask: how to prevent the capillary imbibition of respiratory liquid through a double-layer of cloth mask to improve its effectiveness?

Figure 1 depicts a schematic of the problem. As an impacting respiratory droplet impinges through a two-layer cloth mask [cf. Fig. 1(a)], capillary imbibition of the liquid through the second layer causes the formation of thin liquid layers on the solid parts on the rear-side surface of the second layer. Figure 1(b) shows the proposed design. We seek to evaluate the performance of a double-layer cloth mask in which one layer of high efficiency particulate air (HEPA) filter is inserted between the layers. Using our experiments and analytical models, we will show later in this article that capillary imbibition into a porous medium depends upon the wettability of the material. Due to the hydrophobic nature of the HEPA filter's material as the intermediate layer, the penetrated liquid through the first layer does not undergo capillary imbibition through the HEPA layer, and the rear-side surface of the second-layer remains free of the pathogen-bearing liquid layer, as opposed to the case of Fig. 1(a). On the other hand, as shown later in this article, a single layer of HEPA inhibits impacting droplet penetration through it. Consequently, secondary droplets do not come out. This way, the second layer of the cloth mask remains dry and does not become contaminated with the pathogen-bearing liquid layer. Hence,

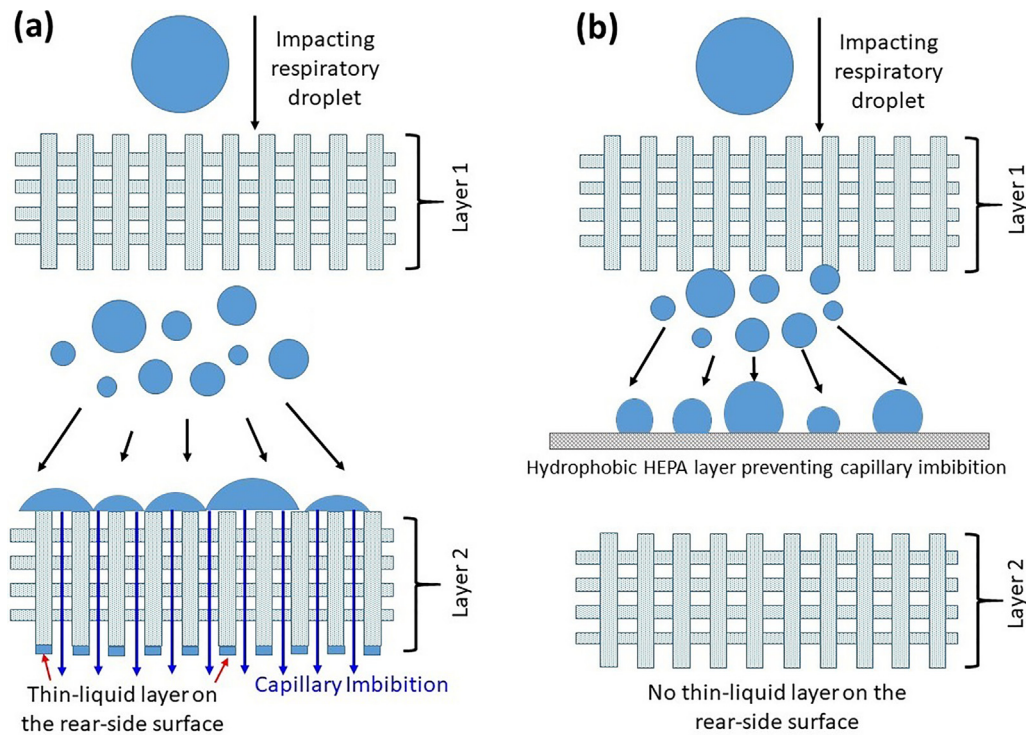


**FIG. 1.** Schematic of the proposed cloth mask design. (a) A two-layer cloth mask, wherein an impacting respiratory droplet first generates smaller secondary droplets after impinging the first layer. After that, the secondary droplets deposit on the second layer and subsequently undergo capillary imbibition through the pores. The imbibition leads to forming a thin liquid layer on the second layer’s rear-side surface, making the surface contaminated. (b) The proposed design, wherein a HEPA filter is inserted between the cloth layers. Due to its hydrophobic nature, it prevents the capillary imbibition of the secondary droplets, leaving the second layer of cloth dry; thereby preventing the rear-side surface from becoming contaminated.

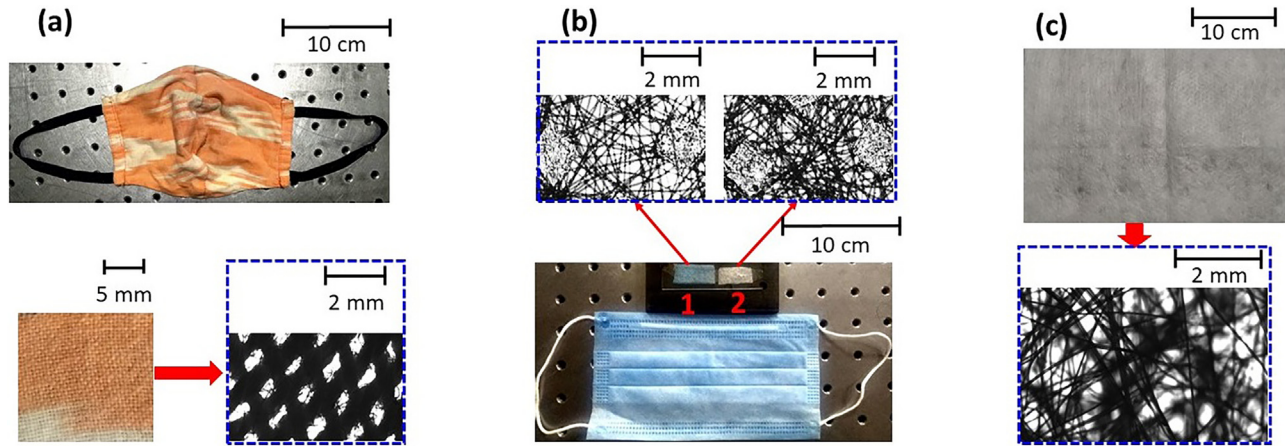
the advantage of the designed cloth masks is twofold. First, it potentially blocks the passage of respiratory liquid through both of the possible routes: one by secondary droplet generation and the other by preventing the capillary imbibition through the intermediate HEPA layer. Second, the HEPA filter is well-known for having the capability to trap particulate matter through electrostatic interaction.<sup>48</sup> Therefore, in addition to impeding the passage of respiratory liquid, the proposed mask may also help impede the passage of pollutants, enabling the user to breathe fresh air. Hence, the proposed mask may serve the dual purpose of protecting the user from pathogens and pollutants. Moreover, the designed mask is comfortable and overcomes the limitations of surgical and N95 masks outlined earlier.

First, we present the characterization of single-layer sample surfaces, i.e., cloth [cf. Fig. 2(a)], each of different layers of the surgical mask [cf. Fig. 2(b)] and HEPA filter [cf. Fig. 2(c)]. The details of the procured materials are given in the [supplementary material](#). To elucidate the characteristic features of the samples, two independent experiments were considered. First, digital image acquisition and optical microscopic visualization of the sample surfaces were carried out to delineate the surface topography. The experimental procedure and data recording details are provided in the [supplementary material](#). Second, we characterize the time-varying shape of a sessile droplet on single-layer sample surfaces to look at the difference in the wettability, evaporation, and capillary imbibition characteristics on these surfaces [cf. Figs. 4 (Multimedia view) and 5 (Multimedia view)]. These

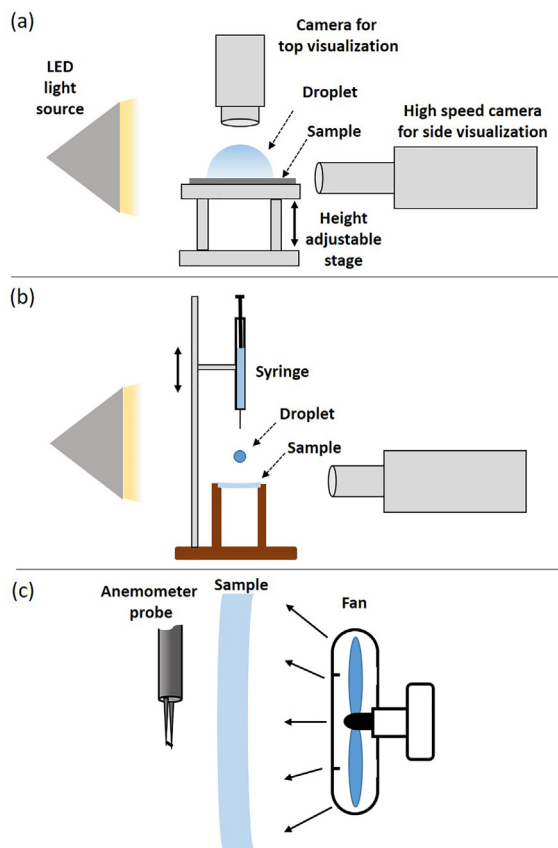
characterizations aid in understanding the contrast in the droplet behavior across different surfaces. After delineating these basic features, the impact and the associated outcomes on single to multilayered mask structures along with the present design will be presented later in this article. The details of the experimentation, data acquisition, and processing procedures are detailed in the [supplementary material](#). Briefly, an initial volume of  $V_0 = 1 \mu\text{l}$  sessile droplet was gently deposited on the surface under investigation, and the temporal variation of droplet geometry was monitored by high-speed visualization from the side and top [cf. Fig. 3(a)]. In all experiments, time  $t = 0$  is considered the instance when the droplet is deposited onto the surface, assuming a spherical cap shape and contact between the droplet and the substrate is established.

Figure 2 depicts the digital and optical microscopic images (within the blue dashed squares) of the samples used. Figure 2(a) shows the images of the cloth mask used in the present study. The mask is composed of two layers of the same cloth material. The microscopic view depicts the typical structure of a woven fabric, also reported earlier.<sup>17</sup> Figure 2(b) shows the images for the surgical mask under consideration. The surgical mask consists of three layers. The outermost layer has a blue color, designated by “1” in Fig. 2(b). The middle and innermost layers are the same and have white color, designated as “2” in Fig. 2(b). Yet, the microscopic images of layers “1” and “2” do not exhibit any qualitative difference. The fibrous structure of surgical mask layers is quite irregular compared to that of cloth.

28 September 2023 14:29:45



**FIG. 2.** Digital photos and optical microscopic images (within the blue dashed square) of the samples used in this study. (a) Cloth mask containing two layers of the same cloth material. (b) Surgical mask containing three layers. The outermost layer has a blue color, designated by “1.” The middle and the innermost layers have white color, designated by “2.” The red arrows indicate the optical microscopic images of the respective layers. The microscopic images do not reveal any qualitative difference between the layers “1” and “2.” (c) HEPA filter.



**FIG. 3.** Experimental setup for the present study depicting different components. (a) High-speed visualization of time-varying droplet geometry in terms of contact angle and wetted diameter on single-layer samples. (b) High-speed visualization of droplet impact and associated phenomenon on single to multiple layer samples. (c) Testing the breathability and comfortability of the proposed design.

Figure 2(c) illustrates the digital image and optical microscopic view of the HEPA filter under consideration. The fibrous structure of the HEPA filter surface is also quite irregular compared to that of the cloth surface.

Next, the second step of sample characterization, i.e., the time-variation of sessile droplet geometry onto the sample surfaces, is presented. Figure 4 (Multimedia view) depicts the temporal variation of droplet geometry in terms of the instantaneous apparent contact angle  $\theta$  and wetted diameter  $D_W$ ; normalized with their respective values  $\theta_0$  and  $D_{W,0}$  on the surfaces of single-layer HEPA, surgical mask layers “1” and “2,” respectively. The frames in Fig. 4 (Multimedia view) show the representative droplet images on HEPA filter surfaces at different times extracted from the high-speed movies. On the droplet image at  $t = 0$ , the definition of  $\theta$  and  $D_W$  is shown. The  $x$ -axis of the plots has been normalized with respect to the droplet lifetimes,  $t_f$  on the surfaces under consideration ( $\sim 800$  s for both the layers of a surgical mask and  $>1500$  s for the HEPA filter). For the HEPA filter, surgical mask blue layer, and surgical mask white layer, the  $\theta_0$  values are  $\sim 120^\circ$ ,  $95^\circ$ , and  $93^\circ$ , respectively. Hence, all of these surfaces are hydrophobic. From Fig. 4 (Multimedia view), we see that for all the surfaces, the droplet liquid does not imbibe through the pores: the bulk droplet resides on the top surface and evaporates. It is widely accepted that evaporation under such conditions can be considered to be diffusion-limited.<sup>49,50</sup> On the HEPA filter surface, the evaporation occurs in the Constant Contact Radius (CCR) mode, i.e., the wetted diameter remains constant and  $\theta/\theta_0$  decreases for the first 100 s. Thereafter, a mixed-mode comprising decaying  $\theta$  and  $D_W$  is observed. Throughout the evaporation process, the droplet maintains the spherical cap shape. For the case of blue and white color surgical mask layers (layers “1” and “2”), the evaporation happens in the CCR mode for the  $\sim 90\%$  of the droplet lifetime. Both  $\theta$  and  $D_W$  exhibit a sharp decrease at the last stage. The microscopic images of the blue and white layers of the surgical masks are qualitatively the same [cf. Fig. 2(b)], and they exhibit similar evaporation dynamics with comparable  $\theta_0$  values [cf. Fig. 4 (Multimedia view)]. From these observations, we conclude that both

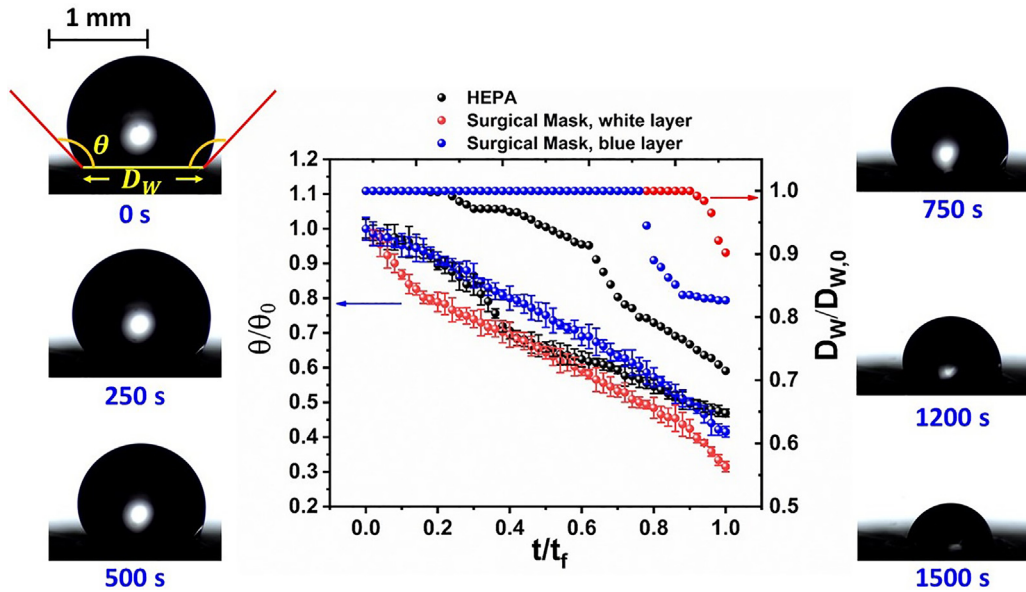


FIG. 4. Temporal variation of contact angle and wetted diameter of  $1 \mu\text{l}$  sessile water droplet on the surfaces of the HEPA filter and different layers of the surgical mask. The images on the left and right columns represent the droplet on the HEPA filter surface at different time frames extracted from the high-speed movies. On the droplet image at time  $t = 0$ , the definition of the apparent contact angle,  $\theta$ , and the wetted diameter  $D_w$  are illustrated. Multimedia view: <https://doi.org/10.1063/5.0094116.1>

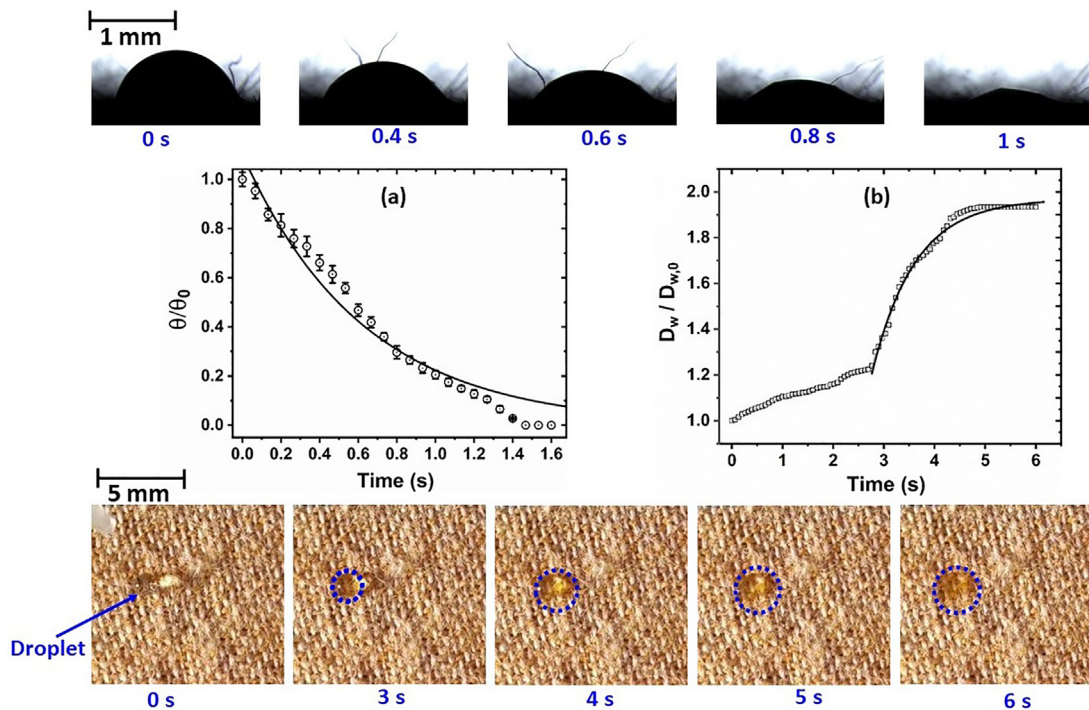


FIG. 5. Temporal evolution of (a) contact angle and (b) wetted diameter of a  $1 \mu\text{l}$  sessile water droplet on a single layer cloth mask surface. The images at the top and bottom rows are the representative views of the droplet at different time frames extracted from the high-speed side and top visualization, respectively. The blue-dashed circles indicate the wetted patch after complete spreading of the droplet. Multimedia view: <https://doi.org/10.1063/5.0094116.2>

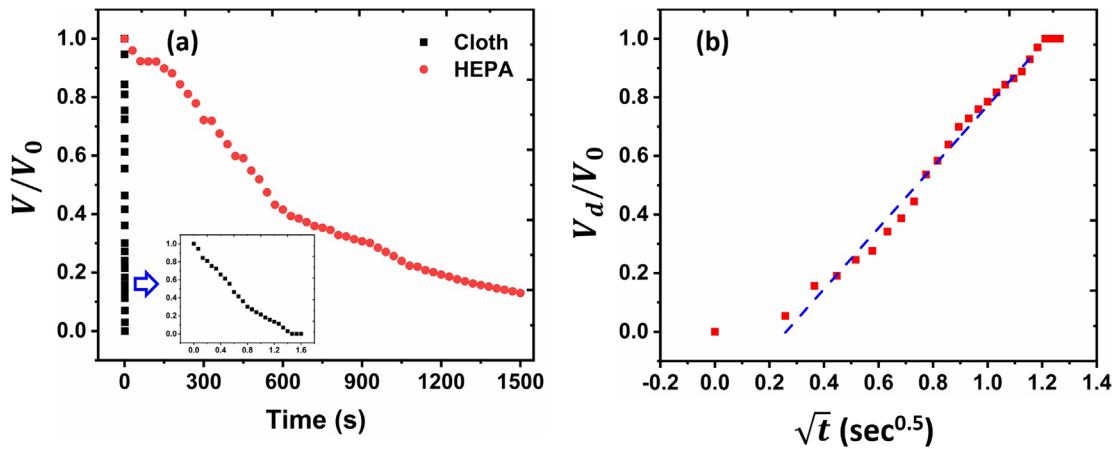


FIG. 6. (a) Temporal evolution of spherical cap droplet volume found from the experiments for the cases of the cloth and HEPA filter surface. The inset shows a magnified plot for the case of cloth for better clarity. (b) Imbibed droplet volume with respect to the square root of time for the case of cloth and comparison with Washburn's equation.

the surgical mask layers are characteristically similar and hereafter will be called “surgical mask surface.”

Next, we investigate droplet interaction with a single-layer cloth. The time-varying droplet shape in terms of  $\theta/\theta_0$  and  $D_W/D_{W,0}$  has been shown in Figs. 5(a) (Multimedia view) and 5(b), respectively. The images at the top and bottom rows are the representative views of the

droplet at different time frames extracted from the high-speed side and top visualization, respectively. We observe a starkly different behavior of the sessile droplet on the cloth as compared to that of the HEPA filter and surgical mask surfaces [cf. Fig. 4 (Multimedia view)]. As seen from Fig. 5 (Multimedia view), on cloth,  $\theta_0 \sim 68^\circ$ ; hence, the substrate is hydrophilic, as opposed to the cases of HEPA and surgical

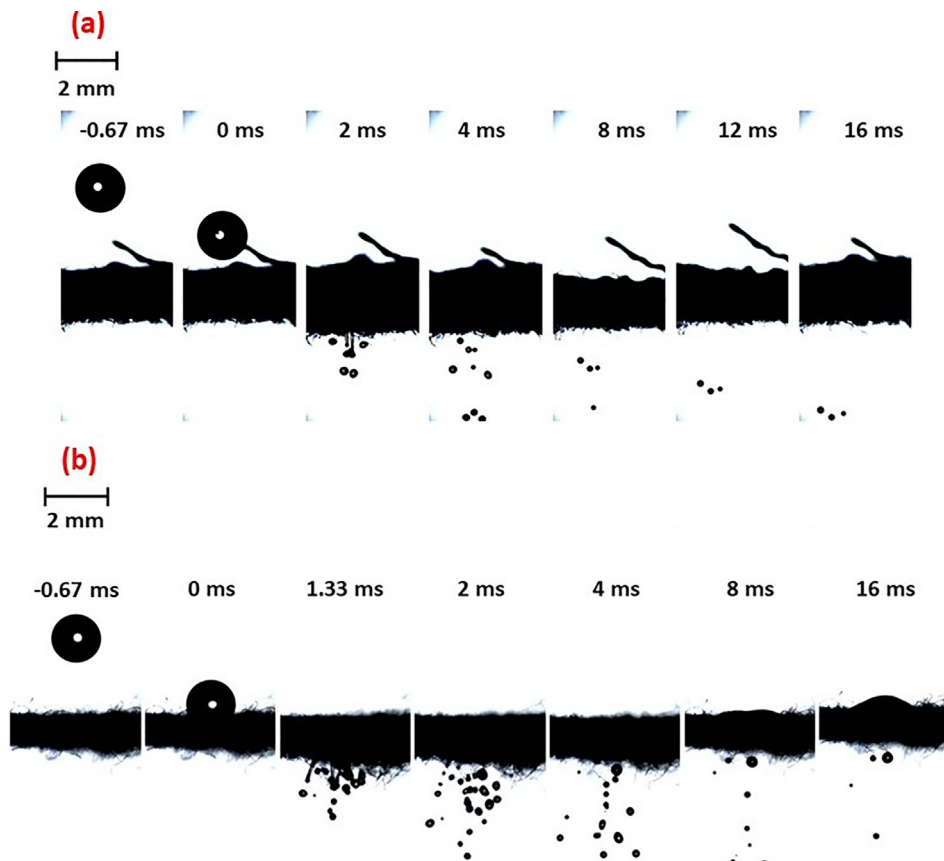


FIG. 7. Impact on a single layer cloth mask and secondary droplet generation for  $We =$  (a) 208 and (b) 416. Multimedia view: <https://doi.org/10.1063/5.0094116.3>

mask surfaces. In addition, the droplet does not simply reside on the top surface to undergo diffusion-limited evaporation. Rather, maintaining its spherical cap geometry, the droplet spreads over the surface, evident from an augmenting wetted diameter. Spreading is caused by the adhesive interaction between the triple-phase contact line and the horizontally oriented fibers on the cloth surface.<sup>51</sup> In addition, capillary imbibition through the pores causes  $\theta$  to decay rapidly.<sup>52,53</sup> After  $t \sim 1.6$  s, the droplet height decays to the extent that it gets hidden within the fibrous structure, making the side-visualization impossible further. However, from the top, we observe the emergence of a wetted patch formed after the complete spreading. At later times ( $t > 6$  s), the wetted patch keeps its area the same and subsequently faints to disappear from the experimental window at  $t \sim 60$  s. The disappearance of the wetted patch can be seen from the Multimedia view associated with Fig. 5, and the frames have not been included in the figure. Similar observations were reported elsewhere<sup>17</sup> for a sessile droplet deposited on a lint-free cloth. Hence, rustic cloth masks respond to respiratory droplets in the same way as lint-free cloths do. From the observations, the key difference between the cloth (hydrophilic) and HEPA filter/surgical mask surfaces (hydrophobic) is that a sessile droplet deposited on cloth undergoes spreading and capillary imbibition, while on HEPA and surgical mask surfaces, it remains on the surface and evaporates, exhibiting neither spreading nor capillary

imbibition. From the time scales depicted in Figs. 4 (Multimedia view) and 5 (Multimedia view), it is understood that the capillary imbibition is a much faster process as compared to the diffusion limited evaporation, which will further be evaluated by spherical-cap volume analysis presented below.

Next, we construct the governing equations to decipher why the sessile droplet exhibits capillary imbibition on cloth but not on the HEPA filter and surgical mask surfaces. Using spherical cap approximation, we evaluate the droplet's instantaneous volume  $[V(t)]$  above the top surface. Under this approximation, if the instantaneous contact angle, droplet height, and wetted radius are  $\theta(t)$ ,  $H_{drop}(t)$ , and  $R_W(t)$  respectively,  $V(t)$  can be obtained as

$$V(t) = \frac{\pi H_{drop}(t)}{6} [3(R_W(t))^2 + (H_{drop}(t))^2], \quad (1)$$

where

$$\tan(\theta(t)/2) = \frac{H_{drop}(t)}{R_W(t)}. \quad (2)$$

$\theta(t)$  and  $R_W(t)$  are found from the experiments [cf. Figs. 4 (Multimedia view) and 5 (Multimedia view)]. Hence, the experimental  $V(t)$  can be obtained.

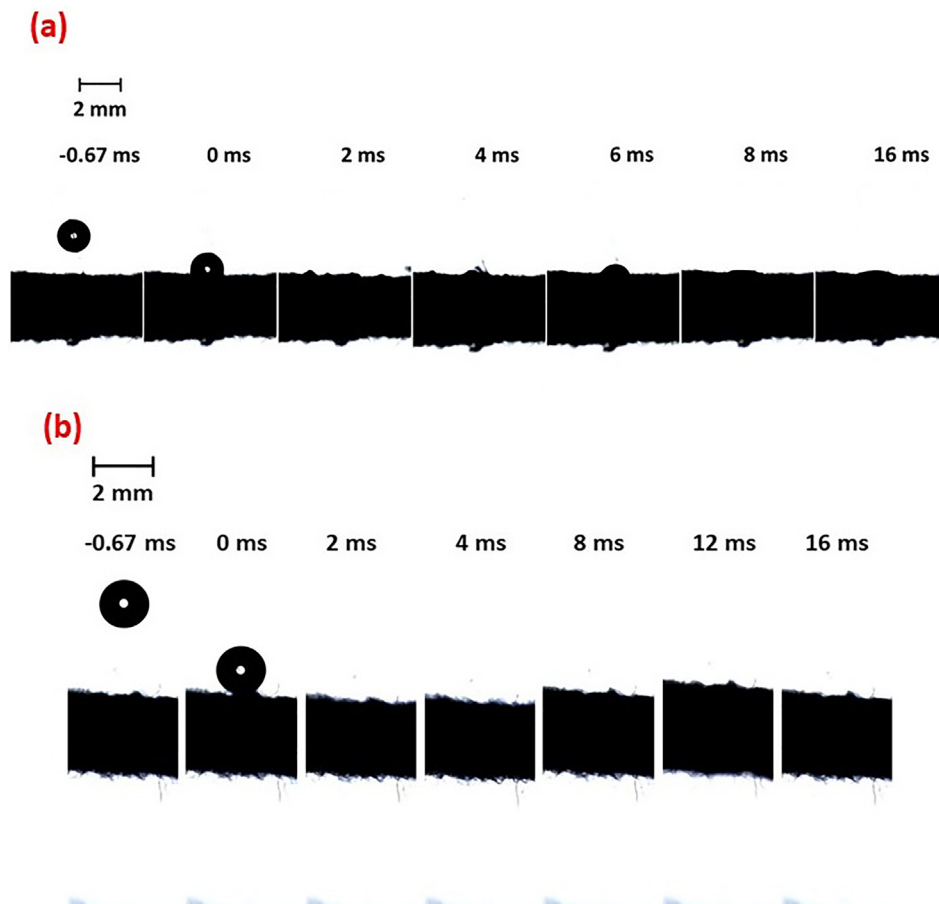


FIG. 8. Impact on a double layer cloth mask for  $We =$  (a) 208 and (b) 416. No secondary droplet ejection was observed. Multimedia view: <https://doi.org/10.1063/5.0094116.4>



Washburn’s equation<sup>54</sup> describes the capillary imbibition phenomenon through the pores by assuming the porous material to be an array of cylindrical capillary tubes. For a liquid of surface tension  $\gamma_{LV}$ , viscosity  $\mu$ , and pore radius  $r$ , the penetration length  $l_p$  of the liquid plug inside a *single* pore at time  $t$  is given by

$$l = \sqrt{\frac{\gamma_{LV} r \cos \theta}{4\mu}} t. \tag{3}$$

Hence, the volume imbibed by a single pore,  $V_{d,1}$ , is given by:<sup>17</sup>

$$V_{d,1} = \pi r^2 \sqrt{\frac{\gamma_{LV} r \cos \theta}{4\mu}} t. \tag{4}$$

Assuming  $\delta_A$  to be the area fraction of the pores, the number of wetted pores ( $n$ ) at time  $t$  is given by  $n = \frac{\pi(R_W(t))^2 \delta_A}{\pi r^2}$ . Hence, the temporal evolution of the drained volume  $V_d(t)$  can be computed as:<sup>17</sup>

$$V_d(t) = nV_{d,1} = \pi(R_W(t))^2 \delta_A \sqrt{\frac{\gamma_{LV} r \cos \theta}{4\mu}} t. \tag{5}$$

Hence, experimentally,  $V_d(t)$  can be computed by the relation  $V_d(t) = V_0 - V(t)$ .

From Eq. (5), it is seen that the imbibed volume  $V_d(t)$  at a time instant is proportional to  $\sqrt{\cos \theta}$ ; hence, the wettability of the underlying porous surface plays a crucial role in determining the imbibition dynamics. For a hydrophobic surface, which is the case for HEPA filter and surgical mask surfaces,  $\theta > \frac{\pi}{2}$ ; hence, by virtue of  $\sqrt{\cos \theta}$ ,  $V_d(t)$  becomes imaginary. Hence, no imbibition would occur on the

hydrophobic surface, and the droplet would remain on the top surface, undergoing diffusion-limited evaporation. This concept corroborates our observation of HEPA filters and surgical mask surfaces. On the other hand, for hydrophilic surfaces, which is the case for the cloth,  $\theta < \frac{\pi}{2}$  and  $V_d(t)$  are real. Hence, continuous imbibition should occur, leaving a thin-liquid layer coverage on both the front and rear surface of the sample, which supports our experimental observations on cloth.

To compare the contrast in the behavior between diffusion-limited evaporation and capillary imbibition, we compare the temporal evolution of droplet volume on the cloth and HEPA filter surface. Figure 6 illustrates the results. From Fig. 6(a), we see that for the HEPA filter surface, the droplet volume decays much more slowly than on the cloth surface. For better clarity, a magnified plot for cloth has been shown in the inset. The spherical cap droplet lifetime on the HEPA filter surface is  $\sim 500$  s. This timescale is consistent with the droplet lifetime on a moderately hydrophobic, impermeable surface, such as stainless steel.<sup>17</sup> Thus, we assert that a sessile droplet on a hydrophobic porous surface undergoes evaporation, not capillary imbibition. Furthermore, from Fig. 6(b), we see that for the case of cloth,  $V_d(t)/V_0$  vs  $\sqrt{t}$  can be well-fitted by a straight line with an adjusted R-square of  $\sim 0.95$ . Hence, the droplet behavior on the hydrophilic cloth obeys Eq. (5) illustrating that capillary imbibition dominates the droplet behavior on the cloth. Therefore, from the above analysis, it is clear that the cloth leads to prominent capillary imbibition among all the materials under consideration due to its hydrophilic nature, while the HEPA filter and surgical mask material inhibit the capillary imbibition due to their hydrophobicity. Hence, consistent with Fig. 1, we envision that while a two-layer cloth mask may prevent ejection of secondary droplets, capillary imbibition of the penetrated

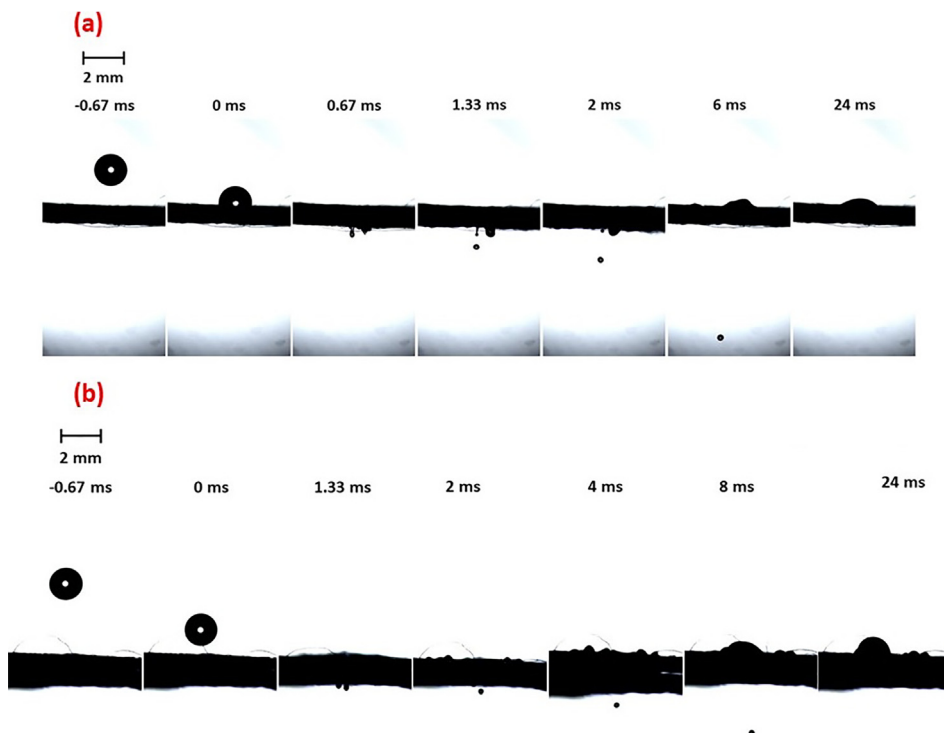


FIG. 9. Impact on a double layer surgical mask and ejection of secondary droplets for  $We =$  (a) 208 and (b) 416. Multimedia view: <https://doi.org/10.1063/5.0094116.5>

28 September 2023 14:29:45

liquid through the second layer would cause the rear-side surface of the second layer to be contaminated with a residual thin-liquid layer. Individuals exposed to the rear-side surface may potentially catch the infection. However, if a HEPA filter is inserted in between the layers of a cloth mask, the hydrophobic intermediate layer would prevent capillary imbibition, thereby inhibiting the passage of respiratory liquid through the designed mask. Next, we present experimental results of the droplet impact on single to multi-layered cloth and surgical masks and evaluate the performance of the proposed design of the HEPA filter insert in a two-layer cloth mask.

For the impact experiments, six different samples were considered: (i) one-layer cloth mask, (ii) two-layer cloth mask, (iii) two-layer surgical mask, (iv) 3-layer surgical mask, (v) one-layer HEPA filter, (vi) a combination of one-layer cloth and one-layer HEPA filter, and (vii) a combination of one-layer surgical and one-layer HEPA filter. Out of these, sample (vi) serves to evaluate the efficiency of the proposed design. As shown below, no secondary droplet ejection and wetting of the rear-side sample surface due to capillary imbibition were recorded for the cases of a single-layer HEPA filter and a combination of one-layer cloth and one-layer HEPA filter. Hence, HEPA filter insertion between the two cloth layers would automatically block the passage of respiratory liquid through the mask. The details of the

experimental setup for the impact experiments are given in the [supplementary material](#). Briefly, a  $D_0 \sim 1.65$  mm-diameter water droplet was allowed to impact the sample held between two supports [cf. [Fig. 3\(b\)](#)]. The droplet was allowed to fall under gravity, and the impact velocity ( $U_0$ ) was varied by varying the impact height. The droplet impact at different velocities was parameterized in terms of the Weber number,  $We$ , which is the ratio between the impact kinetic energy and surface tension and is defined as  $We = \frac{\rho_L U_0^2 D_0}{\gamma_{LV}}$ , where  $\rho_L = 1000$  kg/m<sup>3</sup> is the liquid density and  $\gamma_{LV} = 0.072$  N/m is the liquid surface tension.  $We$  was varied in the range (208, 416), impact at which results in secondary droplet ejection as reported in the previous studies.<sup>43,44</sup>

[Figures 7 \(Multimedia view\)–13 \(Multimedia view\)](#) qualitatively show the droplet impact and the associated consequences (penetration and secondary droplet ejection/no penetration) at different time frames for all the samples (i)–(vii) under consideration. Two representatives,  $We = 208$  (lowest) and 416 (highest), have been chosen for demonstration. The time frames have been extracted from the associated Multimedia views. [Figure 14](#) quantitatively shows the penetrated volume fraction [cf. [Fig. 14\(a\)](#)] and the mean  $We$  of the ejected secondary droplets [cf. [Fig. 14\(b\)](#)] upon impact onto different sample surfaces under consideration. The observations from [Figs. 7 \(Multimedia view\)–14](#) can be summarized as follows. Penetration of

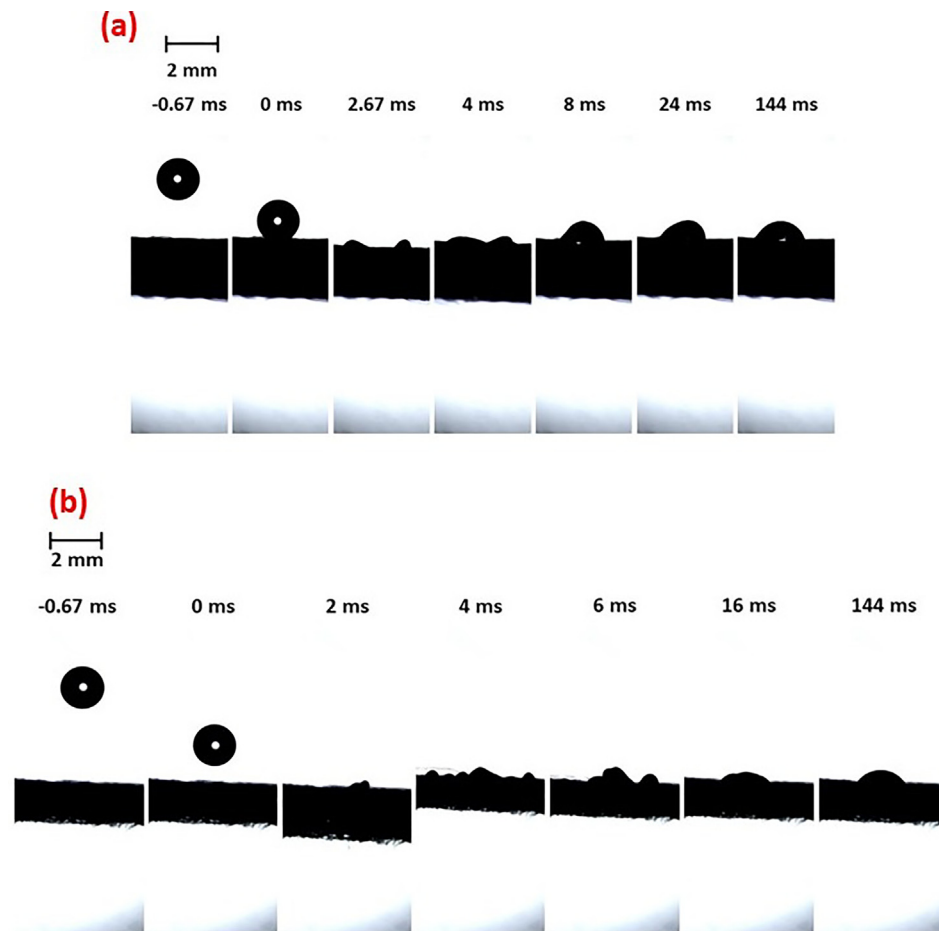


**FIG. 10.** Impact on a triple layer surgical mask for  $We =$  (a) 208 and (b) 416. No secondary droplet ejection was observed. Multimedia view: <https://doi.org/10.1063/5.0094116.6>

liquid and ejection of secondary droplets are observed only for two cases: one-layer cloth mask and two-layer surgical mask. For the rest of the samples, secondary droplet ejection was not observed in the range of  $We$  considered herein. Notably, a single layer HEPA filter potentially prevents liquid penetration and does not allow the ejection of secondary droplets for all  $We$ . Hence, a HEPA filter may be considered a potential candidate for blocking respiratory droplet penetration; a single-layer HEPA filter resists secondary droplet ejection more strongly than a two-layer surgical mask.

Consequently, a combination of a one-layer surgical mask and one-layer HEPA filter; and a one-layer cloth mask and one-layer HEPA filter do not allow the ejection of secondary droplets. Thus, the efficiency of the proposed face mask consisting of a two-layer cloth and an intermediate HEPA filter layer is proven. From Fig. 14, we see that for the cases of one-layer cloth and two-layer surgical masks, the fractional volume of the penetrated liquid and the mean  $We$  of the ejected secondary droplets increase with the impact  $We$  up to  $We = 347$ , which is expected.<sup>43,44</sup> Interestingly, at the highest  $We = 416$ , both the quantities exhibit a slight decrease as compared to their values at  $We = 347$ . The reduction in the penetrated volume fraction and the ejected secondary droplets' mean  $We$  was not observed in the previous studies by Sharma *et al.*,<sup>43</sup> and Krishnan *et al.*<sup>44</sup> We attribute this distinct feature to the flexibility of the sample hung between the two supports at the ends [cf. Fig. 3(b)]. From Figs. 7–13 and the associated Multimedia views, we see that impact at the highest  $We = 416$  induces a significantly large-amplitude oscillation on the

samples as compared to the impact at lower  $We$ . Based upon the knowledge available in the literature,<sup>55</sup> the substrate oscillation, due to its flexibility, induces a recoil kinetic energy onto the droplet. Hence, at large  $We$ , the droplet liquid has a higher tendency to recoil, and the penetrated volume fraction and the associated mean  $We$  of the ejected secondary droplets diminish. In the previous studies by Sharma *et al.*<sup>43</sup> and Krishnan *et al.*,<sup>44</sup> the samples were rigidly fixed at the ends, and therefore, they did not deform as a response to the droplet impact. In our experiments, the samples hung between two supports at the ends are flexible. They significantly oscillate in response to the droplet impact at the highest  $We$ ; hence, the penetration volume diminishes. Indeed, it is visible from Figs. 7–9 and the associated Multimedia views that for the impact at  $We = 416$ , a significant fraction of the droplet volume remains at the top surface even after the penetration and the ejection process of secondary droplets are over. From the observations, it appears that there exists a threshold  $We$  at which the penetrated volume fraction and the mean  $We$  of the ejected droplets are the highest for a flexible porous substrate. Our experimental constraints limit us to increase the impact  $We$  further. Hence, increasing  $We$  further to delineate the threshold as mentioned earlier may be an interesting direction for future research. The flexibility of the mask samples considered herein captures a more realistic scenario as compared to that employed in earlier studies.

From Figs. 7 (Multimedia view), 8 (Multimedia view), and 14, we see that for all  $We$  under consideration, a single-layer cloth mask allows a significant volume of the impacting droplet to penetrate through it

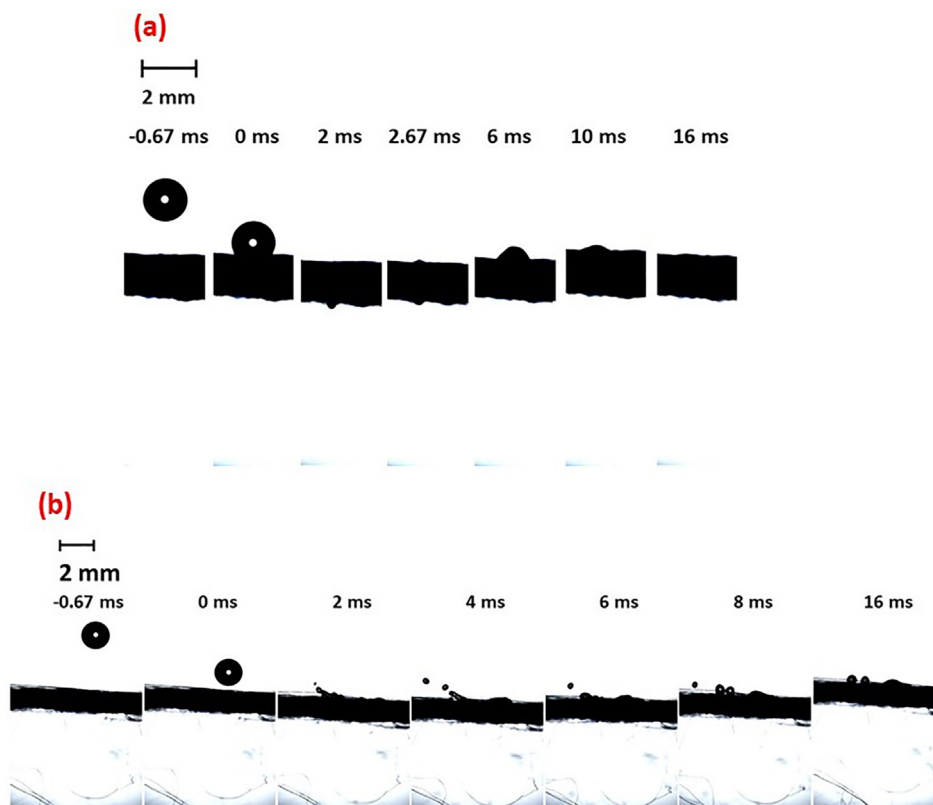
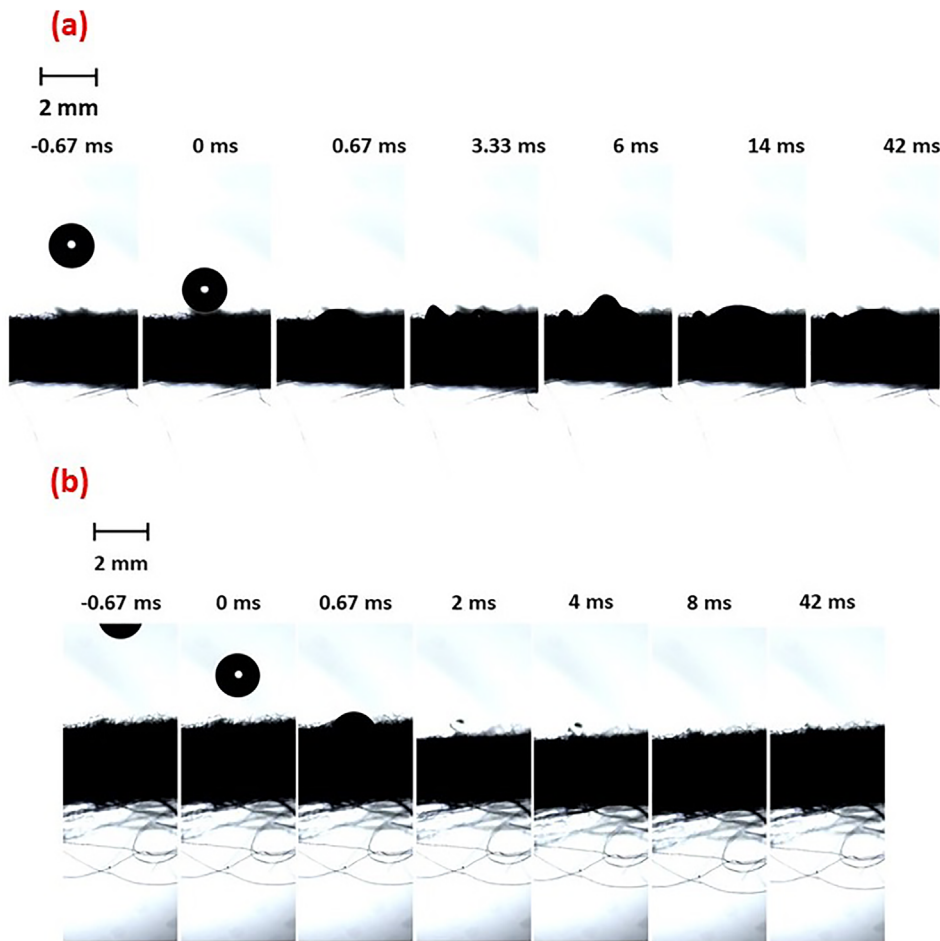


FIG. 11. Impact on a single layer HEPA filter for  $We =$  (a) 208 and (b) 416. No secondary droplet ejection was observed. Multimedia view: <https://doi.org/10.1063/5.0094116.7>



**FIG. 12.** Impact on a combination of one-layer cloth mask and one-layer HEPA filter for  $We =$  (a) 208 and (b) 416. No secondary droplet ejection was observed. Multimedia view: <https://doi.org/10.1063/5.0094116.8>

generating secondary droplet ejection from the rear-side, while a two-layer cloth mask prevents penetration of liquid and the associated generation of secondary droplets. However, as depicted schematically in Fig. 1, although the liquid propagation is slowed down during passage through a double-layer cloth mask, capillary imbibition of the droplet-liquid through the second layer causes the formation of a thin-layer of pathogen-bearing liquid on the rear-side surface of the second layer. On the other hand, a single layer HEPA filter neither causes the ejection of secondary droplets [cf. Fig. 11 (Multimedia view)] nor allows capillary imbibition through it [cf. Fig. 4 (Multimedia view)]. Hence, the HEPA filter insert should block any respiratory liquid passage through a double-layer cloth mask. To further reassure this concept, we performed more experiments by impacting a droplet dyed with  $\text{KMnO}_4$  onto the surfaces of a two-layer cloth mask, one-layer HEPA filter, and 3-layer surgical mask. Figure 15 shows the results. In Fig. 15, the “front” and “rear” sides, respectively, represent the side at which the impact is performed and the side opposite to the impact. Figure 15(a) shows the front and rear sides of a two-layer cloth mask after impact at  $We = 208$  and 416. We observe that the droplet impact on the front side surface leads to liquid propagation at the rear side surface. Hence, the secondary droplets that are ejected from the first layer are imbibed through the second layer and a liquid

layer emerges at the rear-side surface. For the cases of the one-layer HEPA filter and 3-layer surgical masks [cf. Figs. 15(b) and 15(c)], we see that the impacted droplet remains at the top surface of the front layer. The dye spots visible at the rear sides are just the signatures of the dye that resides on the front surface. The contrast in the intensity of the dye spots seen in the front and the rear sides along with the visual observation that the fibers at the rear side are oriented at the top of the surface above the visible dye spots conclusively demonstrates that the impacted liquid does not propagate to the rear side surface of the sample. Hence, the performance of a single-layer HEPA filter in blocking a respiratory fluid is comparable to that of a three-layer surgical mask. However, due to the fibrous structure, a single HEPA filter cannot be worn, and hence, we recommend inserting an intermediate HEPA filter layer between the two cloth layers.

Finally, we evaluate the breathability and comfortability of the designed mask. The details of the experimental procedure are outlined in the supplementary material. Briefly, the decay in the airflow speed through the mask was measured by a hot wire anemometer [cf. Fig. 3(c)]. A desk fan was employed to generate a flow of air, and the anemometer probe was kept at a distance of 25 cm from it. The sample was kept at a mid-way between the fan and the anemometer probe. In

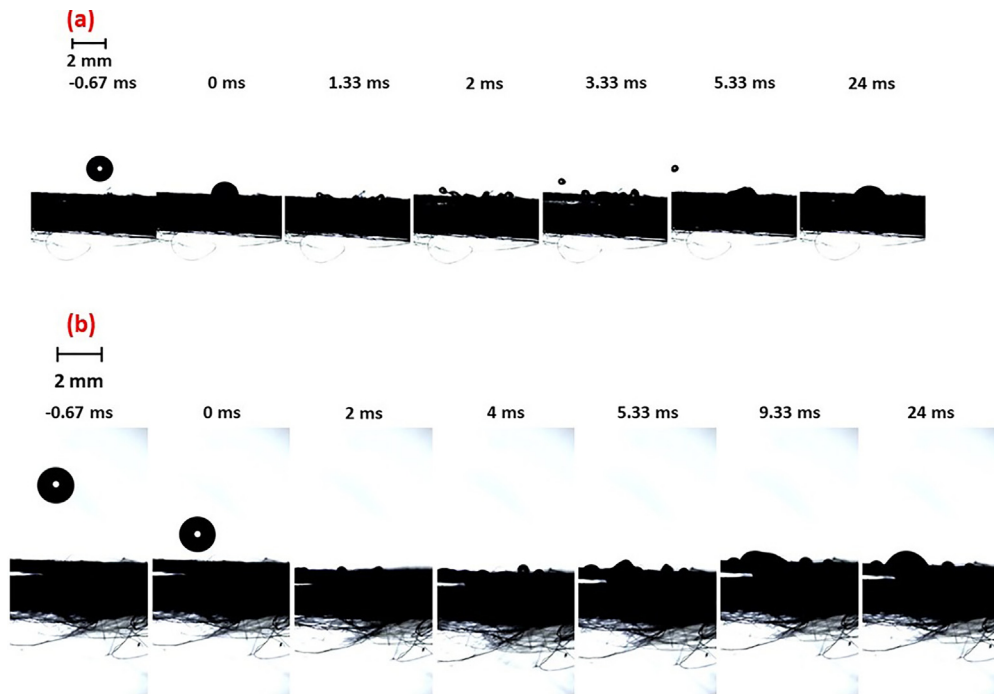


FIG. 13. Impact on a combination of a one-layer surgical mask and one-layer HEPA filter for  $We = (a)$  208 and  $(b)$  416. No secondary droplet ejection was observed. Multimedia view: <https://doi.org/10.1063/5.0094116.9>

these experiments, the samples chosen were two-layer cloth masks, 3-layer surgical masks, one-layer HEPA filter, and a two-layer cloth mask with an intermediate HEPA filter layer. Figure 16(a) shows the method of obtaining the airflow profile after different experimental runs for a representative case of a two-layer cloth mask with an intermediate HEPA filter layer, which is the designed face mask reported in

this study. At the time  $t = 0$ , the fan is switched on. The detected airflow speed increases rapidly to reach an asymptotic value. However, the profile at the steady-state exhibits obvious noises. We obtained the detected airflow speed vs time for different experimental runs, and the average of these curves was taken. After that, the obtained average was smoothed to remove noise to get a clear, discernable trend. The

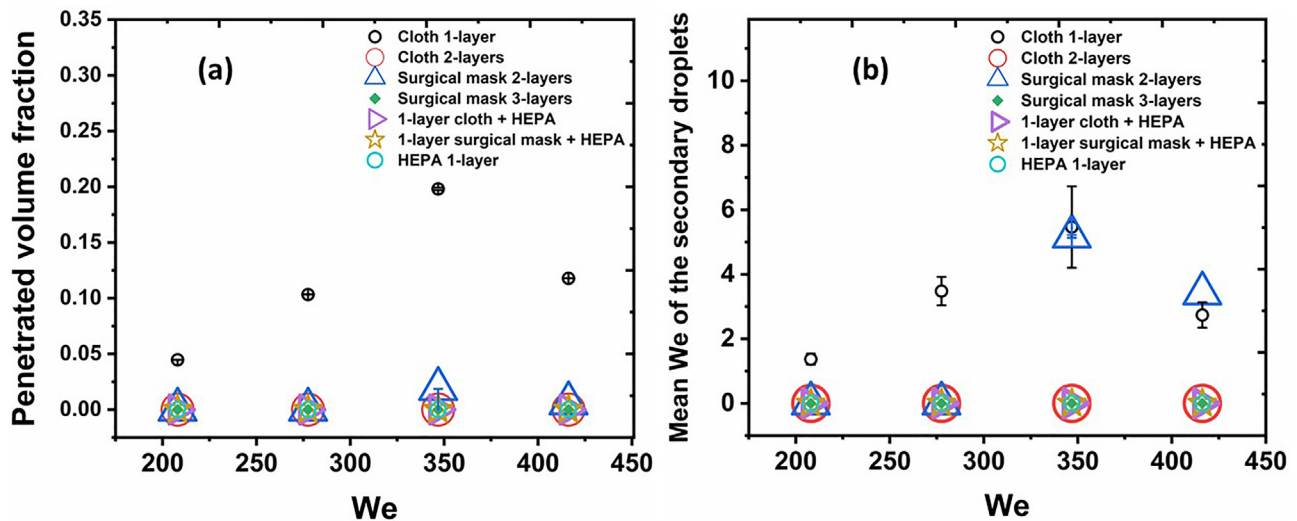


FIG. 14. (a) Volume fraction of penetrated liquid and (b) mean  $We$  of the ejected secondary droplets with respect to the impact of  $We$  for different samples under consideration.

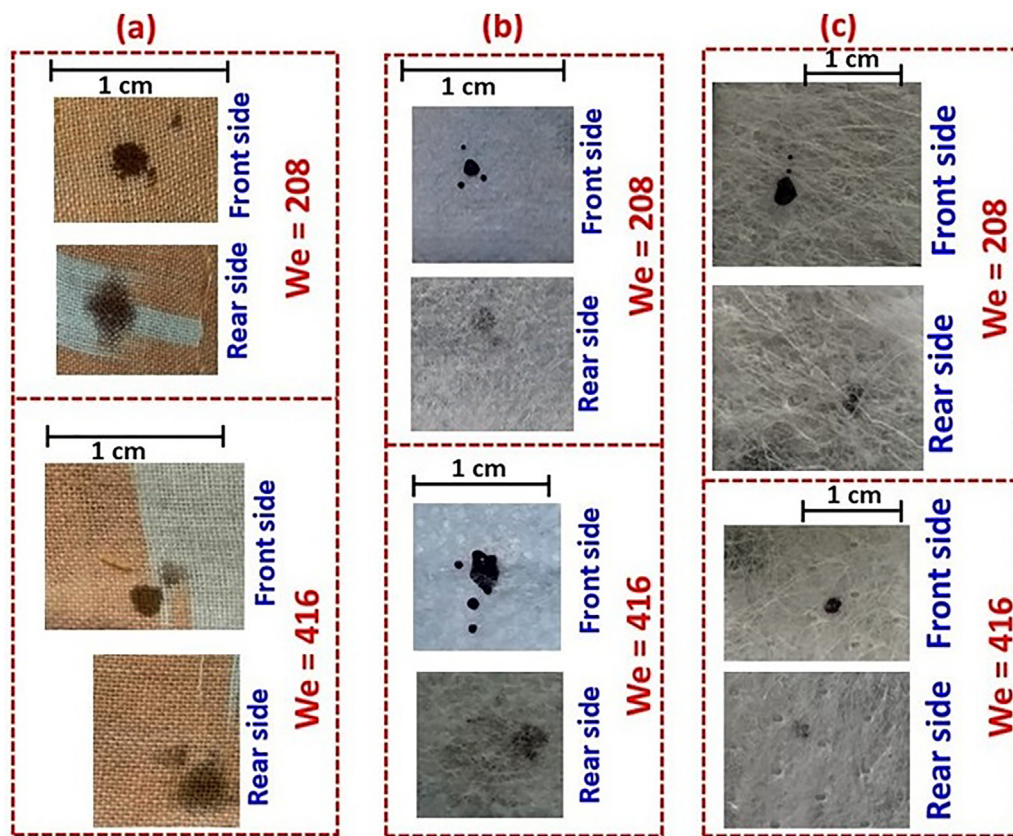


FIG. 15. Examining the liquid penetration on the rear-side surface of (a) two-layer cloth mask, (b) 3-layer surgical mask, and (c) single layer HEPA filter after the impact of a droplet dyed with  $\text{KMnO}_4$ .

smoothing was carried out with the help of the adjacent-averaging method embedded in the Origin<sup>®</sup> software, which essentially takes the average of a user-specified number of data points (5 chosen herein) around each point in the data and replaces that point with the new average value. The final curve obtained after averaging and smoothing is shown by the thick black curve in Fig. 16(a). This way, the average air-flow speed profiles were obtained for all the samples, and the results are shown in Fig. 16(b). As expected, direct exposure, i.e., without any sample, the detected speed remains the highest. In the presence of the samples, single layer HEPA allows the highest amount of air to pass through it. For the respective cases of the surgical mask (3-layers), cloth mask (two-layers), and a two-layer cloth mask with an intermediate HEPA layer, essentially, the same amount of air passes through the samples. Hence, we conclude that the HEPA filter inserted into a double-layer cloth mask does not deteriorate the mask's breathability and comfortability. This way, the desired performance of the proposed face mask design has been evaluated.

In conclusion, we attempt to improve the effectiveness of makeshift cloth masks to mitigate the spread of COVID-19. Cloth masks available to date have the least ability to prevent the passage of infectious respiratory droplets through it compared to the other popular masks, namely, surgical and N95 masks. However, surgical masks are

not snugly-fit, thus causing significant leakage. The synthetic fibers reduce comfortability and are not desired by allergic individuals who suffer from facial eczema. Moreover, the N95 mask causes excessive  $\text{CO}_2$  inhalation and reduces heat transfer in the nose. Given this fact, we seek to improve the efficiency of a two-layer cloth mask by introducing an intermediate HEPA layer. A single-layer cloth mask allows a significant volume of the impacting droplet to penetrate through it, ejecting secondary droplets from the rear side. However, the droplet impact on a two-layer cloth mask does not lead to the secondary droplet ejection. Notably, despite slowing down the liquid penetration and preventing the secondary droplet generation, capillary imbibition through woven fabrics causes the liquid to be transported to the second layer forming a thin-liquid layer at the rear-side surface of the mask and contaminating it. The hydrophilic nature of cloth triggers the capillary imbibition. Conversely, the insertion of the intermediate HEPA filter layer prevents the capillary imbibition through it, making the second cloth layer free of pathogen-bearing liquid. The impedance to the imbibition by the intermediate HEPA filter layer has been attributed to its hydrophobic characteristics. We experimentally and analytically assess the role of wettability in governing the capillary imbibition mechanism. Finally, the designed two-layer cloth mask with an intermediate HEPA filter layer has been tested for breathability and

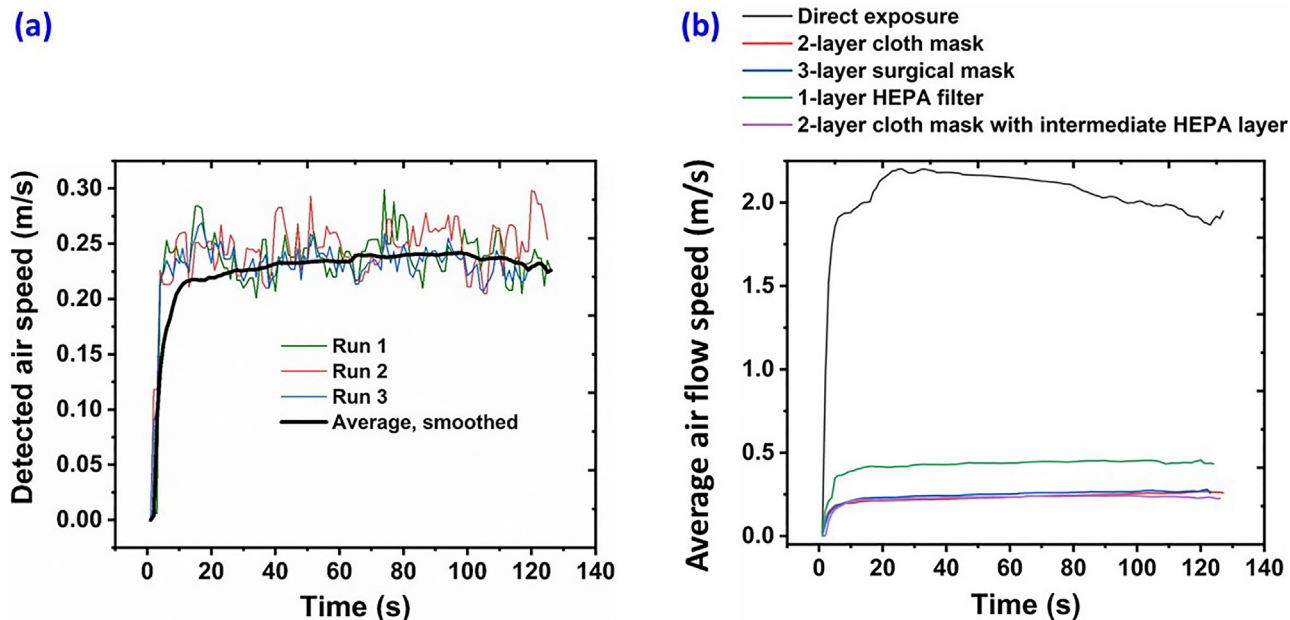


FIG. 16. Measurement of airflow speed after the generated airflow passes through different samples. (a) Method for obtaining the airspeed profile for several experimental runs shown for a representative case of the cloth mask with the HEPA filter inserted between the layers. (b) Airspeed vs time plot for different samples. Time  $t = 0$  corresponds to the time when the fan is switched on.

comfortability. The findings are, therefore, useful from fundamental viewpoints as well as to contain the spread of diseases, which spreads through respiratory droplets, such as COVID-19 and influenza.

See the [supplementary material](#) for schematic and details of the experimental procedure and supporting results.

We gratefully acknowledge financial support of an internal grant from the Industrial Research and Consultancy Centre (IRCC), IIT Bombay. R.B. thanks Professor Rajat Mittal at Johns Hopkins University for a useful discussion on HEPA insert in a face mask at the onset of the COVID-19 pandemic.

## AUTHOR DECLARATIONS

### Conflict of Interest

The authors have no conflicts to disclose.

## DATA AVAILABILITY

The data that support the findings of this study are available from the corresponding author upon reasonable request.

## REFERENCES

- <sup>1</sup>S. Chaudhuri, S. Basu, P. Kabi, V. R. Unni, and A. Saha, "Modeling the role of respiratory droplets in COVID-19 type pandemics," *Phys. Fluids* **32**, 063309 (2020).
- <sup>2</sup>X. April Si, M. Talaat, and J. Xi, "SARS CoV-2 virus-laden droplets coughed from deep lungs: Numerical quantification in a single-path whole respiratory tract geometry," *Phys. Fluids* **33**, 023306 (2021).
- <sup>3</sup>S. P. Bhat, B. R. Kumar, S. R. Kalamkar, V. Kumar, S. Pathak, and W. Schneider, "Modeling and simulation of the potential indoor airborne transmission of SARS-CoV-2 virus through respiratory droplets," *Phys. Fluids* **34**, 031909 (2022).
- <sup>4</sup>Y. Yang, Y. Wang, L. Tian, C. Su, Z. Chen, and Y. Huang, "Effects of purifiers on the airborne transmission of droplets inside a bus," *Phys. Fluids* **34**, 017108 (2022).
- <sup>5</sup>R. Biswas, A. Pal, R. Pal, S. Sarkar, and A. Mukhopadhyay, "Risk assessment of covid infection by respiratory droplets from cough for various ventilation scenarios inside an elevator: An openfoam-based computational fluid dynamics analysis," *Phys. Fluids* **34**, 013318 (2022).
- <sup>6</sup>M. Kanso, J. Piette, J. Hanna, and A. Giacomini, "Coronavirus rotational diffusivity," *Phys. Fluids* **32**, 113101 (2020).
- <sup>7</sup>M. Kanso, V. Chaurasia, E. Fried, and A. Giacomini, "Peplomer bulb shape and coronavirus rotational diffusivity," *Phys. Fluids* **33**, 033115 (2021).
- <sup>8</sup>C. C. Wang, K. A. Prather, J. Sznitman, J. L. Jimenez, S. S. Lakdawala, Z. Tufekci, and L. C. Marr, "Airborne transmission of respiratory viruses," *Science* **373**, eabd9149 (2021).
- <sup>9</sup>S. K. Das, J.-e. Alam, S. Plumari, and V. Greco, "Transmission of airborne virus through sneezed and coughed droplets," *Phys. Fluids* **32**, 097102 (2020).
- <sup>10</sup>A. Agrawal and R. Bhardwaj, "Reducing chances of COVID-19 infection by a cough cloud in a closed space," *Phys. Fluids* **32**, 101704 (2020).
- <sup>11</sup>A. K. Mallik, S. Mukherjee, and M. V. Panchagnula, "An experimental study of respiratory aerosol transport in phantom lung bronchioles," *Phys. Fluids* **32**, 111903 (2020).
- <sup>12</sup>M. Z. Bazant and J. W. Bush, "A guideline to limit indoor airborne transmission of COVID-19," *Proc. Natl. Acad. Sci.* **118**, e2018995118 (2021).
- <sup>13</sup>S. Chatterjee, J. S. Murallidharan, A. Agrawal, and R. Bhardwaj, "How coronavirus survives for hours in aerosols," *Phys. Fluids* **33**, 081708 (2021).
- <sup>14</sup>S. Behera, R. Bhardwaj, and A. Agrawal, "Effect of co-flow on fluid dynamics of a cough jet with implications in spread of COVID-19," *Phys. Fluids* **33**, 101701 (2021).
- <sup>15</sup>R. Bhardwaj and A. Agrawal, "Likelihood of survival of coronavirus in a respiratory droplet deposited on a solid surface," *Phys. Fluids* **32**, 061704 (2020).
- <sup>16</sup>R. Bhardwaj and A. Agrawal, "How coronavirus survives for days on surfaces," *Phys. Fluids* **32**, 111706 (2020).

- <sup>17</sup>S. Chatterjee, J. S. Murallidharan, A. Agrawal, and R. Bhardwaj, "Why coronavirus survives longer on impermeable than porous surfaces," *Phys. Fluids* **33**, 021701 (2021).
- <sup>18</sup>S. Chatterjee, J. S. Murallidharan, A. Agrawal, and R. Bhardwaj, "Designing antiviral surfaces to suppress the spread of COVID-19," *Phys. Fluids* **33**, 052101 (2021).
- <sup>19</sup>P. Katre, S. Banerjee, S. Balusamy, and K. C. Sahu, "Fluid dynamics of respiratory droplets in the context of covid-19: Airborne and surface-borne transmissions," *Phys. Fluids* **33**, 081302 (2021).
- <sup>20</sup>D. Lewis *et al.*, "COVID-19 rarely spreads through surfaces. so why are we still deep cleaning," *Nature* **590**, 26–28 (2021).
- <sup>21</sup>S. Chatterjee, J. S. Murallidharan, A. Agrawal, and R. Bhardwaj, "A review on coronavirus survival on impermeable and porous surfaces," *Sādhanā* **47**, 1–13 (2022).
- <sup>22</sup>See <https://www.who.int/emergencies/diseases/novel-coronavirus-2019/advice-for-public> for "Advice for the public: Coronavirus disease (COVID-19)" (2022).
- <sup>23</sup>T. Dbouk and D. Drikakis, "On respiratory droplets and face masks," *Phys. Fluids* **32**, 063303 (2020).
- <sup>24</sup>D. Mirikar, S. Palanivel, and V. Arumuru, "Droplet fate, efficacy of face mask, and transmission of virus-laden droplets inside a conference room," *Phys. Fluids* **33**, 065108 (2021).
- <sup>25</sup>V. Arumuru, J. Pasa, and S. S. Samantaray, "Experimental visualization of sneezing and efficacy of face masks and shields," *Phys. Fluids* **32**, 115129 (2020).
- <sup>26</sup>A. Khosronejad, S. Kang, F. Wermelinger, P. Koumoutsakos, and F. Sotiropoulos, "A computational study of expiratory particle transport and vortex dynamics during breathing with and without face masks," *Phys. Fluids* **33**, 066605 (2021).
- <sup>27</sup>S. Kumar and H. P. Lee, "The perspective of fluid flow behavior of respiratory droplets and aerosols through the facemasks in context of Sars-CoV-2," *Phys. Fluids* **32**, 111301 (2020).
- <sup>28</sup>S. Verma, M. Dhanak, and J. Frankenfield, "Visualizing the effectiveness of face masks in obstructing respiratory jets," *Phys. Fluids* **32**, 061708 (2020).
- <sup>29</sup>A. Agrawal and R. Bhardwaj, "Probability of COVID-19 infection by cough of a normal person and a super-spreader," *Phys. Fluids* **33**, 031704 (2021).
- <sup>30</sup>I. Rios de Anda, J. W. Wilkins, J. F. Robinson, C. P. Royall, and R. P. Sear, "Modeling the filtration efficiency of a woven fabric: The role of multiple length scales," *Phys. Fluids* **34**, 033301 (2022).
- <sup>31</sup>P. Prasanna Simha and P. S. Mohan Rao, "Universal trends in human cough airflows at large distances," *Phys. Fluids* **32**, 081905 (2020).
- <sup>32</sup>V. Arumuru, S. S. Samantaray, and J. Pasa, "Double masking protection vs. comfort—A quantitative assessment," *Phys. Fluids* **33**, 077120 (2021).
- <sup>33</sup>S. Sarkar, A. Mukhopadhyay, S. Sen, S. Mondal, A. Banerjee, P. Mandal, R. Ghosh, C. M. Megaridis, and R. Ganguly, "Leveraging wettability engineering to develop three-layer DIY face masks from low-cost materials," *Trans. Indian Nat. Acad. Eng.* **5**, 393–398 (2020).
- <sup>34</sup>T. Oberg and L. M. Brosseau, "Surgical mask filter and fit performance," *Am. J. Infection Control* **36**, 276–282 (2008).
- <sup>35</sup>See <https://allergyasthmanetwork.org/news/face-masks-facial-eczema> for "Face masks and facial eczema: What you can do" (2022).
- <sup>36</sup>W. Hua, Y. Zuo, R. Wan, L. Xiong, J. Tang, L. Zou, X. Shu, and L. Li, "Short-term skin reactions following use of N95 respirators and medical masks," *Contact Dermatitis* **83**, 115–121 (2020).
- <sup>37</sup>See <https://www.uhhospitals.org/Healthy-at-UH/articles/2020/09/what-to-do-about-skin-problems-caused-by-face-masks> for "What to do about skin problems caused by face masks" (2022).
- <sup>38</sup>J. Lan, Z. Song, X. Miao, H. Li, Y. Li, L. Dong, J. Yang, X. An, Y. Zhang, L. Yang *et al.*, "Skin damage among health care workers managing coronavirus disease-2019," *J. Am. Acad. Dermatol.* **82**, 1215–1216 (2020).
- <sup>39</sup>D. M. Elston, "Occupational skin disease among health care workers during the coronavirus (COVID-19) epidemic," *J. Am. Acad. Dermatol.* **82**, 1085–1086 (2020).
- <sup>40</sup>H. Salati, M. Khamooshi, S. Vahaji, F. C. Christo, D. F. Fletcher, and K. Inthavong, "N95 respirator mask breathing leads to excessive carbon dioxide inhalation and reduced heat transfer in a human nasal cavity," *Phys. Fluids* **33**, 081913 (2021).
- <sup>41</sup>E. Koroteeva and A. Shagiyanova, "Infrared-based visualization of exhalation flows while wearing protective face masks," *Phys. Fluids* **34**, 011705 (2022).
- <sup>42</sup>R. Bhardwaj and A. Agrawal, "Tailoring surface wettability to reduce chances of infection of COVID-19 by a respiratory droplet and to improve the effectiveness of personal protection equipment," *Phys. Fluids* **32**, 081702 (2020).
- <sup>43</sup>S. Sharma, R. Pinto, A. Saha, S. Chaudhuri, and S. Basu, "On secondary atomization and blockage of surrogate cough droplets in single-and multilayer face masks," *Sci. Adv.* **7**, eabf0452 (2021).
- <sup>44</sup>B. Krishan, D. Gupta, G. Vadlamudi, S. Sharma, D. Chakravorty, and S. Basu, "Efficacy of homemade face masks against human coughs: Insights on penetration, atomization, and aerosolization of cough droplets," *Phys. Fluids* **33**, 093309 (2021).
- <sup>45</sup>B. Kumar, S. Chatterjee, A. Agrawal, and R. Bhardwaj, "Evaluating a transparent coating on a face shield for repelling airborne respiratory droplets," *Phys. Fluids* **33**, 111705 (2021).
- <sup>46</sup>T. Dbouk and D. Drikakis, "Weather impact on airborne coronavirus survival," *Phys. Fluids* **32**, 093312 (2020).
- <sup>47</sup>T. Dbouk and D. Drikakis, "Fluid dynamics and epidemiology: Seasonality and transmission dynamics," *Phys. Fluids* **33**, 021901 (2021).
- <sup>48</sup>P. Barn, E. Gombojav, C. Ochir, B. Laagan, B. Beejin, G. Naidan, B. Boldbaatar, J. Galsuren, T. Yambaa, C. Janes *et al.*, "The effect of portable HEPA filter air cleaners on indoor pm2.5 concentrations and second hand tobacco smoke exposure among pregnant women in Ulaanbaatar, Mongolia: The UGAAR randomized controlled trial," *Sci. Total Environ.* **615**, 1379–1389 (2018).
- <sup>49</sup>M. Kumar and R. Bhardwaj, "A combined computational and experimental investigation on evaporation of a sessile water droplet on a heated hydrophilic substrate," *Int. J. Heat Mass Transfer* **122**, 1223–1238 (2018).
- <sup>50</sup>S. Chatterjee, M. Kumar, J. S. Murallidharan, and R. Bhardwaj, "Evaporation of initially heated sessile droplets and the resultant dried colloidal deposits on substrates held at ambient temperature," *Langmuir* **36**, 8407–8421 (2020).
- <sup>51</sup>E. Ezzatneshan and R. Goharimehr, "Study of spontaneous mobility and imbibition of a liquid droplet in contact with fibrous porous media considering wettability effects," *Phys. Fluids* **32**, 113303 (2020).
- <sup>52</sup>X. Frank and P. Perre, "Droplet spreading on a porous surface: A lattice Boltzmann study," *Phys. Fluids* **24**, 042101 (2012).
- <sup>53</sup>S. Das, H. Patel, E. Milacic, N. Deen, and J. Kuipers, "Droplet spreading and capillary imbibition in a porous medium: A coupled IB-VOF method based numerical study," *Phys. Fluids* **30**, 012112 (2018).
- <sup>54</sup>I. Melciu and M. Pascovici, "Imbibition of liquids in fibrous porous media," in *IOP Conference Series: Materials Science and Engineering* (IOP Publishing, 2016), Vol. 147, p. 012041.
- <sup>55</sup>G. Upadhyay, V. Kumar, and R. Bhardwaj, "Bouncing droplets on an elastic, superhydrophobic cantilever beam," *Phys. Fluids* **33**, 042104 (2021).